Korean J. Chem. Eng., **30**(4), 796-812 (2013)
DOI: 10.1007/s11814-012-0218-6

New emissions targeting strategy for site utility of process industries

Mohamamd Hasan Khoshgoftar Manesh*, Sajad Khamis Abadi, Majid Amidpour*†, Hooman Ghalami**, and Mohammad Hosein Hamedi***

*Energy & Process Integration Research Center, Department of Energy Systems Engineering, Faculty of Mechanical Engineering, K. N. Toosi University of Technology, Tehran, Iran
**Department of Energy Engineering, Science and Research Branch, Islamic Azad University, Tehran, Iran
(*Received 9 August 2012 • accepted 16 December 2012*)

Abstract−A new procedure for environmental targeting of co-generation system is presented. The proposed method is based on the concepts of pinch technology for total site targeting of fuel, power, steam, environmental impacts and total annualized cost with considering emissions taxes. This approach provides a consistent, general procedure for determining mass flow rates and efficiencies of the applied turbines. This algorithm utilizes the relationship of entropy with enthalpy and isentropic efficiency. Also, the life cycle assessment (LCA) as a well-known tool for analyzing environmental impacts on a wide perspective with reference to a product system and the related environmental and economic impacts have been applied. In this regard, a damage-oriented impact analysis method based on Eco-indicator 99 and footprints analysis was considered. In addition, the present work demonstrates the effect of including both sensible and latent heating of steam in the extended Site Utility Grand Composite Curve (ESUGCC). It is shown that including sensible heating allows for better thermal matching between the processes. Furthermore, the other representation Y-SUGCC as the other form of Site Utility Grand Composite has been proposed. Two case studies were used to illustrate the usefulness of the new environmental targeting method.

Key words: Environemtal Targeting, Total Annulized Cost, Cogeneration, Total Site, New Procedure

INTRODUCTION

Chemical processes usually require steam at different pressure and temperature values for heating and non-heating purposes. To provide steam in the required condition, the designer has to decide whether to provide steam in the extreme condition and then reduce it to different levels or produce steams separately in different boilers. Many industrial processes operate within total sites [1-3], where they are serviced and linked through a common central utility system. This utility system meets the demands for heat and power of individual process units by indirect heat integration. However, greater benefits in terms of energy and capital cost can be obtained by looking at the entire site. Total site integration addresses the task of optimizing each process and utility system in the context of the overall site [3].

A number of models have been proposed for the early estimation of cogeneration for utility systems using steam turbines. Dhole and Linnhoff [1] proposed an exergetic model based on the site source-sink profiles. Raissi [2] presented the T-H model based on the Salisbury approximation, assuming power to be linearly proportional to the difference between the inlet and outlet saturation temperatures.

Klemes et al. [3] proposed a novel methodology that can reduce energy demands and emissions on a total factory site while simultaneously avoiding loss of cogeneration efficiency. This approach takes into account the specific features of semi-continuous and batch operations and also the opportunities offered by the multi-objective optimization of the design strategy for the total site. The environmental costs and potential for regulatory action were also incorporated [3]. Sorin and Hammache [4] developed an exergetic model based on thermodynamic insights for the Rankine cycle and showed that power was not linear in saturation temperature differences.

Mavromatis and Kokossis [5] introduced the non-linear model of THM (turbine hardware model) based on the principle of the Willian's line in order to incorporate variation of efficiency with turbine size and operating load. Harell [6] introduced a graphic technique for estimating the cogeneration potential which utilizes the concept of extractable power and header efficiency in order to establish cogeneration potential. Varbanov et al. [7] developed the improved turbine hardware model. Mohan and El-Halwagi [8] presented a linear algebraic approach based on the concept of extractable power and steam main efficiency.

Medina-Flores and Picon-Nunez [9] proposed a modified thermodynamic model by keeping the advantages of the THM. Bandyopadhyay et al. [10] developed a linear model based on the Salisbury approximation and energy balance at steam mains. A new shaft work targeting model, called the Iterative Bottom-to-Top Model (IBTM), was presented by Ghannadzadeh et al. [11,12]. Kapli et al. [13] introduced a new method for estimating cogeneration potential of site utility systems by a combination of bottom-up and top-down procedures.

Varbanov et al. [14] proposed an extension of the total site methodology covering industrial, residential, service, business and agricultural customers and the incorporation of renewable energy sources, accounting for the often substantial variability on the supply and demand sides and for the use of non-isothermal utilities.

†To whom correspondence should be addressed.
E-mail: amidpour@kntu.ac.ir

Liew et al. [15] introduced four new contributions: (1) Total site sensitivity table (TSST), a tool for exploring the effects of plant shutdown or production changes on heat distribution and utility generation systems over a Total Site; (2) a new numerical tool for TSHI, the total site problem table algorithm (TS-PTA), which extends the well-established problem table algorithm (PTA) to total site analysis; (3) a simple new method for calculating multiple utility levels in both the PTA and TS-PTA; and (4) the total site utility fistribution (TSUD) table, which can be used to design a total site utility distribution network.

Varebanov et al. proposed total site heat recovery targeting using multiple ΔT_{min} specifications for the site processes and process-utility interfaces. It is also possible to define and use the ΔT_{min} contributions of individual process streams in a process [16].

Foder et al. [17] focused on extending traditional total site integration methodology to produce more meaningful utility and heat recovery targets for the process design. This methodology was a further development of a recently extended traditional pinch methodology. The previous extension was on the introduction of using an individual minimum temperature difference (ΔT_{min}) for different processes so that the ΔT_{min} is more representative of the specific process. Further, it deals with stream specific ΔT_{min} inside each process by setting different ΔT contribution (ΔT_{cont}) and also using different ΔT_{cont} between the process streams and the utility systems.

Hackl et al. [18] demonstrated how heat integration tools such as total site analysis and exergy analysis can be applied to target for shaft work and hot utility savings for processes and utility systems operating below ambient temperature.

Rozali et al. [19] extended the graphical and numerical power pinch analysis (PoPA) method by considering the energy losses that occur in the power system conversion, transfer and storage.

Furthermore, Nemet et al. [20] proposed the capital cost targeting method for total site heat recovery to determine the lower bound on the heat transfer area for meeting the targeted heat recovery on the total site.

In recent years, public concern about climate change has grown significantly. Emissions of greenhouse gases such as carbon dioxide, methane and nitrous oxide from industrial activities have long been known to be major contributors to global warming [21]. This trend has led to significant interest in the increased use of energy technologies with inherently low-carbon footprints as well as in retrofitting of existing ones (to reduce greenhouse gas emissions [3,21].

There has been increased research in the development of new modeling techniques to analyze and simulate the effects of these technologies on carbon emissions, and furthermore to optimize the deployment of appropriate technologies in order to meet environmental goals while simultaneously considering technical and economic constraints.

A significant contribution to the CO_2 emitted to the atmosphere is attributed to fossil fuel combustion, which accounts for almost 94.4% of total CO_2 emissions in the US for the year 2010 (EPA, 2012) [22,23].

To meet the environmental regulations, the chemical process industries are challenged to reduce their greenhouse emissions, in particular CO_2 emissions. Site utility of process industries is without doubt the most energy-intensive sector utilized in practice [3], [23, 24]. Therefore, targeting of greenhouse emissions in a steam network is very important.

Also, nitrogen oxides are inorganic chemical compounds where a link between nitrogen and oxygen is formed. The most frequent nitrogen oxides in the air are nitro-monoxide (NO) and nitro-dioxide (NO_2) usually common labeled as NO_x. There are some other nitrogen oxides in the air, from which the most polluting one is nitrous-suboxide (N_2O). Others, such as N_2O_3, N_2O_4, N_2O_5, NO_3, are not contained in the air in greater quantities [24,25].

In addition, life cycle assessment (LCA) as a well-known tool for environmental impacts evaluation and analyses on a wide perspective with reference to a product system and the related environmental and economic impacts has been applied. The quantification of environmental impacts caused by depletion and emissions of a natural resource can be carried out using different life cycle impact assessment methods [26,27]. LCA is a technique for assessing the environmental aspects associated with a product over its life cycle. The LCA process consists of goal definition and scoping (defining the system under consideration), inventory analysis (identifying and quantifying the consumption and release of materials), and interpretation (evaluation of the results) [26,27].

In addition, pinch analysis concepts were extended to applications involving management of CO_2 emissions from industrial systems. Tan et al. proposed the first approach on the use of pinch analysis for carbon-constrained energy sector planning, or in short, carbon emission pinch analysis (CEPA) [28]. The basic technique has then been applied for energy planning purposes in Ireland and New Zealand [29-31].

Bandyopadhyay et al. introduced a novel decomposition algorithm to solve the segregated targeting problem based on the concept of carbon intensity as the quality index for energy streams [32].

Lee et al. reformulate the CEPA targeting technique as a linear programming model that minimizes the amount of zero- or low-carbon sources in an automated way. In addition, the concept of segregated targeting was introduced, in which not all energy sources can be used interchangeably by the demands [33].

The planning of minimal retrofit of power plants for carbon capture and storage was introduced, whereby pinch analysis was proposed to determine the minimum extent of retrofit needed across regional power plants in order to meet an overall carbon footprint target [34].

Tijan et al. [35] extended the CEPA approaches for evaluating and visualizing carbon footprint reduction options in chemical processes.

Several tools for footprint evaluation were presented by Cucek [36], including some of the numerous carbon footprint calculators, available calculators for other footprints, some ecological footprints-based, graph-based, and mathematical programming tools.

A new graphical technique based on pinch analysis is proposed by Ooi et al. to address the planning problem of the storage of captured CO_2 from power plants into corresponding reservoirs [37].

Furthermore, Cucek et al. [38] proposed the potential of total site process integration in order to reflect the key environmental footprints, including carbon, water, and nitrogen footprints. It has been a first step in this direction - towards balancing and reducing key environmental footprints within TSs. Using the obtained indicator values, engineers can more easily decide on the directions of potential improvements to the sites within various site processes as well

as in the utility system [38].

We propose an environmental targeting method for estimation of cogeneration potential, environmental impacts and TAC with considering emission taxes. The pervious works cited do not not have high accuracy for estimation of cogeneration potentials. In this paper, an accurate method has been applied for estimation of shaft work, steam demand in boiler and steam generating and used in each steam main. Also, LCA assessment has been performed based on estimation of Eco-indicator 99, carbon, water, energy and emission foot prints for environmental targeting in site utility.

METHODOLOGY

1. Preparation of SUGCC

The new approach uses the site utility grand composite curve (SUGCC), which represents another form of the site composite curves [39]. The SUGCC was obtained from the site composite curves by representing each steam main on temperature-enthalpy axes by its saturation temperature and steam generation and usage loads, from the source and sinks profiles of the site composites. The differences between steam generation and steam usage set the VHP demand or the supply heat available at each main [39]. The model calculates the minimum required flow rate from a steam generation unit and the levels of superheat in each steam main based on the heat loads specified by SUGCC. Fig. 1 shows a schematic of the utility system layout on SUGCC diagram. More details of Total Site methodology and its related topics are found in Ref. [39].

2. Targeting Cogeneration Potential

In this step, an accurate cogeneration targeting procedure has been applied based on a general procedure for determining the mass flow rates and the efficiencies of the turbines used. The model allows targeting shaftwork production, mass flow and degree of superheat at steam boiler with high accuracy.

Fig. 2 demonstrates the mass balance for i-th steam main. As shown, the L given steam mains are indexed by i from the highest pressure steam main, meaning that i is equal to 1, 2, 3 and 4 for very high pressure (VHP), high pressure (HP), medium pressure (MP) and low pressure (LP) steam mains. There is an expansion zone between two steam mains. Each zone is indexed by Z starting from the top, i.e., Z=1 is for VHP-HP, and one single steam turbine is placed in each zone.

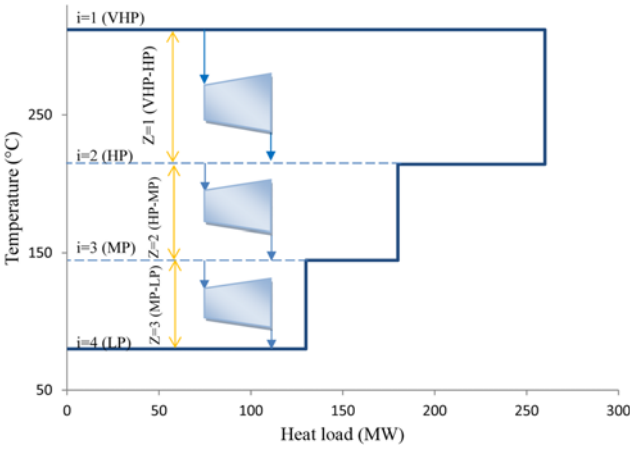

Fig. 1. Schematic of the utility system layout on SUGCC.

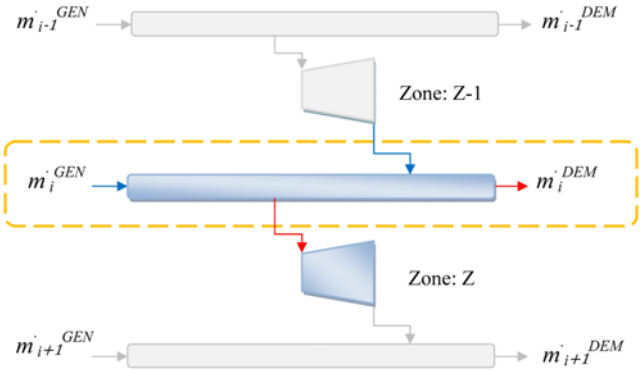

Fig. 2. Mass load balance for i-th steam main.

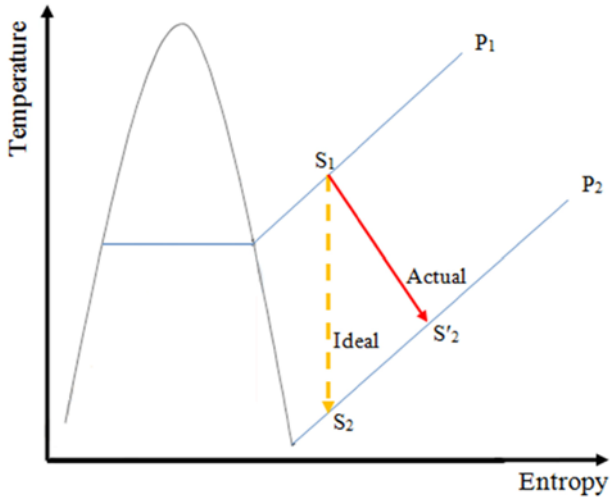

Fig. 3. Thermodynamic expansion of steam at two different pressure levels on a temperature-entropy diagram.

Fig. 3 shows the thermodynamic expansion of steam at two different pressure levels on a temperature-entropy diagram. The step S_1-S_2 shows an isentropic expansion. An isentropic process is an ideal case in which there is no kind of irreversibility, such as mechanical friction and heat losses. Step S_1-S_2 is a better representation of what happens in reality. The outlet of the turbine is shifted to the right side, which indicates the increase of entropy (state of disorder) caused by losses [40]. The isentropic efficiency is basically the ratio of the enthalpy difference of step S_1-S_2 to that of step S_1-S_2.

The isentropic efficiency is a function of the load and, for the fixed values of flow rates, it would be better to consider the highest efficiency, assuming to use turbines, for which the calculated flow rate will be the full load [40]. Varbanov et al. [7], used a thermodynamic model to estimate the isentropic efficiency as follows:

$$\eta_{is} = \frac{W_{max}}{W_{is,max}} \quad (1)$$

where A and B are constants that depend on the turbine and are functions of the saturation temperature. A and B are calculated by Eqs. (2) and (3).

$$A = b_0 + b_1 . \Delta T_{sat} \quad (2)$$

Table 1. The regression coefficients used in the isentropic efficiency equation

	Back pressure turbines		Condensing turbines	
	W_{max}≤2000 kW	W_{max}>2000 kW	W_{max}≤2000 kW	W_{max}>2000 kW
a_0 (kW)	0	0	0	−463
a_1 (kW/°C)	1.08	4.23	0.662	3.53
a_2	1.097	1.155	1.191	1.22
a_3 (°C^{-1})	0.00172	0.000538	0.000759	0.000148

$$B=b_2+b_3.\Delta T_{sat} \tag{3}$$

The values of these constants are given in Table 1.

At the boiler exit, for a given pressure and steam temperature, the enthalpy can be obtained with the aid of steam tables. The actual input enthalpy of steam mains are usually provided from the calculations of the previous steam mains. The input isentropic enthalpy of steam mains is obtained in the superheated region. Then, the efficiency is calculated. The actual enthalpy, which will serve as the input enthalpy for the next zone, is then calculated by using the isentropic enthalpies and efficiency by Eq. (4).

$$h_{i,act}=h_{i-1,is}-\eta(h_{i-1,is}-h_{i,is}) \tag{4}$$

In this study, the superheat temperature at each steam level was calculated by using an iterative procedure based on a certain desirable amount of superheat in the LP steam main. The degree of superheat in the LP steam main needed to be set at 10 to 20 °C [41]. If the degree of superheat in the resulting LP steam main was less than the required level, then operating conditions of VHP would be updated and iterated until the acceptable superheated conditions would be met for the LP steam main.

The mass flow rate of steam expanding through the Z-th turbine ($\dot{m}_z$) can be calculated by the mass balance for i-th by Eq. (5), as shown in Fig. 3:

$$\dot{m}_z=\dot{m}_{z-1}-\dot{m}_i^{DEM}+\dot{m}_i^{GEN} \tag{5}$$

where $\dot{m}_i^{GEN}$ is the flow rate of steam generated by the process and $\dot{m}_i^{DEM}$ is the flow rate of steam demanded by the process, which can be calculated by Eqs. (6) and (7) :

$$\dot{m}_i^{DEM}=\frac{\dot{Q}_i^{DEM}}{h^{act}-h_{f,i}} \tag{6}$$

$$\dot{m}_i^{GEN}=\frac{\dot{Q}_i^{GEN}}{h_i^{act}-h_{f,i}} \tag{7}$$

Here, $h_{f,i}$ denotes the enthalpy of the saturated liquid at the pressure of i-th steam main. Also,

$$\dot{m}_{z,init}=\frac{\dot{Q}_{net,i}}{h_i-h_{f,i}} \tag{8}$$

$$\dot{Q}_{net,i}=\dot{Q}_i^{DEM}-\dot{Q}_i^{GEN} \tag{9}$$

In the next step as shown in Fig. 4, the initial mass flow rates ($\dot{m}_{z,init}$) passing through each zone, assuming isentropic expansions throughout the levels via Eq. (8), are estimated.

The efficiency is modified for improved accuracy using the following expression Eq.(10):

$$\eta_{is}=\frac{1}{B}\left(1-\frac{3.41443\times10^6 A}{\Delta h_{is} M^{max}}\right) \tag{10}$$

In addition, for the given steam levels, the values for h_i and $\dot{m}_i^{NET}$ are revised for better accuracy.

For subsequent iterations through to convergence, the steps are repeated until the stopping criterion is achieved according to the following (Fig. 4):

$$\sqrt{\Sigma_{i=1}^{z}(\dot{m}_z-\dot{m}_{z,new})^2}\le\varepsilon \tag{11}$$

When the first loop of the algorithm terminates, the LP superheat temperature is checked. If it falls below the allowed minimum, the superheat temperature of the boiler is increased and the steps are repeated until the desired amount of superheat is achieved in the LP steam main.

The shaft work production in each zone of the site utility is calculated by Eq. (12):

$$W_z=\dot{m}_z(h_i-h_{i+1}) \tag{12}$$

In this step, the following parameters are determined:

(1) actual steam temperature at each level;
(2) steam flows in each zone
(3) mass flow rate and temperature of steam boiler;
(4) shaft power generation in each zone

3. Environmental Targeting

In this section, environmental targeting based on estimation of greenhouses emissions, carbon and, water, energy and emission footprints and Eco-indicator 99 has been performed as shown in Fig, 4.

3-1. Estimation of GHG Emissions

In the combustion of fuels, air is assumed to be in excess to ensure complete combustion, so that no carbon monoxide is formed. CO_2 emissions, $[CO_2]_{Emiss}$ (kg/s), are related to the amount of fuel burnt, Q_{Fuel} (kW), in a heating device as follows:

$$[CO_2]_{Emiss}=\left(\frac{Q_{Fuel}}{NHV}\right)\left(\frac{C\%}{100}\right)\alpha \tag{13}$$

where α (=3.67) is the ratio of molar masses of CO_2 and C, while NHV (kJ/kg) represents the net heating value of a fuel with a carbon content of C% (-). A carbon tax of 15 $/ton of CO_2 is assumed [23]. Eq. (13) shows that the types of both the fuel used and the heating device affect the amount of CO_2 produced. The heating device influences emissions through the amount of fuel burnt, which is directly related to its efficiency or performance. However, the effect of the fuel can be seen in the terms C%, NHV, and α. These effects can be lumped in the so-called *fuel factor*, $Fuel_{Fact}$ (kg/kJ), defined as Eq. (14):

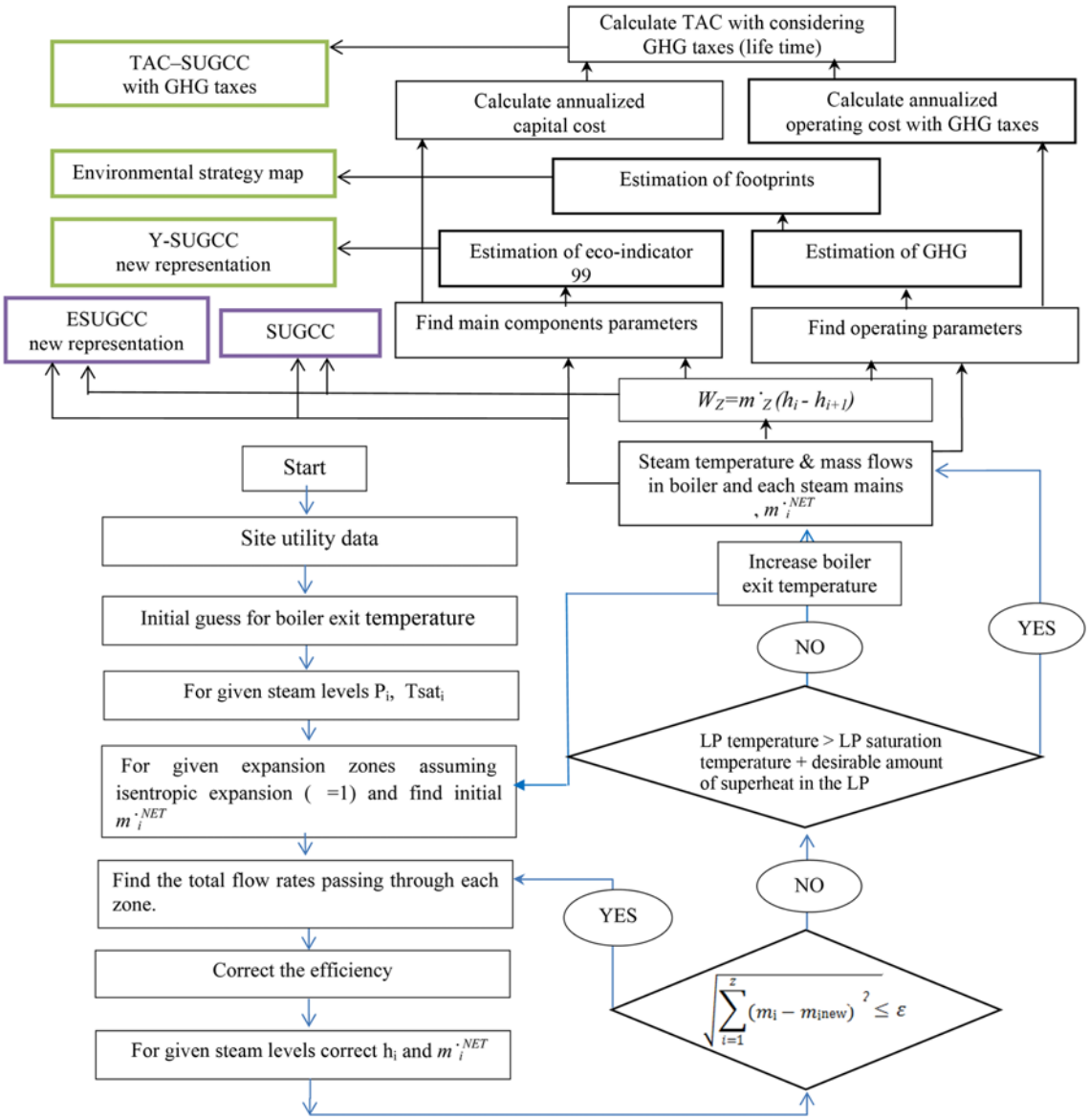

Fig. 4. Algorithm of new environmental targeting.

$$Fuel_{Fact}=\left(\frac{\alpha}{NHV}\right)\left(\frac{C\%}{100}\right) \quad (14)$$

The EPA has established the AP-42 Compilation of Air Pollutant Emission Factors. As indicated in AP-42 [22] standardized emission factor used to calculate nitrogen oxides is 0.057129804 (kg/GJ) and carbon monoxide is 0.014175064 (kg/GJ) from industrial boilers. Knowing the fuel heating values, these emission factors can be converted to mass fractions of tones NO_x emitted per one ton burned fuel. Unit damage costs of CO and NO_x are assumed to 0.02086 $/kg CO and 6.853 $/kg NO_x [24].

3-2. Footprint

Different methods have been developed in the last few years to correlate environmental sustainability of specific activities with land and water areas required to supply this activity with resources and to absorb its wastes [35-38,42,43]. This paper focuses on carbon, energy water and emission footprints.

3-2-1. Carbon Footprint

Recently, the carbon footprint (CF) has become one of the most important environmental protection indicators [36]. It usually stands for the amount of CO_2 and other greenhouse gases (GHGs) emitted over the full life cycle of a process or product. CF demonstrates the quantities of GHGs. A specific time horizon is considered, usually 100 years [36].

For the purpose of environmental targeting, this paper refers to a land-based definition, where the carbon footprint estimates the land area required to sequester atmospheric fossil CO_2 emissions through afforestation to target the maximum area available. This area is calculated as [44]:

$$CF=M_{CO_2}\times\frac{1-F_{CO_2}}{S_{CO_2}}\times EF \quad (15)$$

where CF is the footprint of indirect land occupation by fossil fuel and cement related CO_2 emissions (m^2 y), M_{CO_2} is the product specific

Table 2. Environmental impact functions of components for the construction phase

Component	Environmental impact function, Y_k (Pts of eco-indicator 99)
Steam turbine	$\dot{Y}_{ST}=(189.7+0.2677\times m_s-3.675\times P_{in}-0.0002562\times m_s^2+0.008919\times m_s\times P_{in}+0.022\times P_{in}^2)\times\frac{704\times CRF}{8000}$ $\dot{Y}_{ST}$: Environmental impact function of back pressure steam turbine (Pts/h) m_s: Mass flow of steam (kg/s) P_{in}: Inlet pressure (bar)
Boiler	$\dot{Y}_{Boiler}=(21.76+9.928\times m_s-87.14\times m_f)\times\frac{104\times CRF}{8000}$ $\dot{Y}_{Boiler}$: Environmental impact function of boiler (Pts/h) m_s: Mass flow of steam (kg/s) m_f: Mass flow of fuel (kg/s)

emission of CO_2 (kg CO_2), F_{CO_2} is the fraction of CO_2 absorbed by the oceans, S_{CO_2} is the sequestration rate of CO_2 by biomass (kg CO_2 m^{-2} y^{-1}) and EF is the equivalence factor for forests. This footprint unit of measure is expressed in m^2 [44]. In this step, the CF has been calculated to environmental targeting as shown in Fig. 4. In the targeting phase we can set max area available (m^2).

3-2-2. Emission Footprint

The emission footprint (EMF) demonstrates the quantity of product or service-created emissions into the air (e.g., SO_2, particles, CO, CO_2), water (e.g., chemical oxygen demand (COD), nitrogen and phosphorus), and soil (through spillage in the soil) [44]. EMFs are calculated on a per-area basis. The conversion of emissions is calculated according to the principle that anthropogenic mass flows must not alter the qualities of local compartments [36,44]. More details about emission footprints are found in Ref. [36,44].

3-2-3. Energy Footprint

The energy footprint takes into account different energy supplies as related to different demand categories, such as heating and hot water production, process energy, electricity and traffic [44]. The footprint is calculated by multiplying the final energy use of different energy carriers with their land need indices and adding these results to the footprint of the whole energy supply. This footprint unit of measure is m^2. The details of description and calculation of the water footprint are found in Ref. [36,44]. Max area available (m^2) can be set in design phase.

3-2-4. Water Footprint

The water footprint is related to the concept of virtual water. Virtual water is the amount of water required to produce a service or a product. In analogy with ecological and carbon footprints, this indicator is determined to summarize the contribution of a product or activity to the deterioration of the environment. The focus is on the consumption of the limited resource, water. More details about description and calculation of water footprint are found in Ref. [36,44]. Average water required for a specific category of product or service (m^3) can be set in environmental targeting phase.

3-3. Eco-indicator 99

An LCA is used to assess the environmental impact associated with a product over its lifetime [45] and it is carried out following the guidelines of international standard approaches (ISO 14004) [45, 46]. The quantification of environmental impacts caused by depletion and emissions of a natural resource can be carried out by using different life cycle impact assessment methods. The damage-oriented impact analysis method, Eco-indicator 99, is considered here [46,47]. Eco-indicator 99 defines three categories of damage: (1) damage to human health, (2) damage to the ecosystem and (3) depletion of resources. After the environmental effects of the different categories are calculated, the values are optionally normalized, weighted and the result is expressed in Eco-indicator points (Pts).

Depending on the attitude and perspective of different societies, there is a weighting per perspective represented by three archetypes [45,46]. The archetype of the hierarchists has been adopted in this paper. The standard eco-indicator 99 inventory values are available for the production and processing of a large number of materials, for transport processes, for disposal scenarios, etc [46].

To shift from the manufactured materials to the raw substances and emissions inventory, the software Package Sima Pro 7.1 [47] was used. Also, the data collected were generalized in the form of equations (Table 2) and used for estimating the component-related environmental impact that occurs during the construction phase.

For the LCA of the system being analyzed, we assumed in analogy with the economic analysis a lifetime of 30 years and 8,600 working hours per year at full capacity.

$\dot{Y}_k$ is the environmental impact that occurs during the three life-cycle phases: construction $\dot{Y}_k^{CO}$, operation and maintenance, $\dot{Y}_k^{OM}$, and disposal $\dot{Y}_k^{DI}$ constitute the component-related environmental impact associated with the kth component $\dot{Y}_k$:

$$\dot{Y}_k=\dot{Y}_k^{CO}+\dot{Y}_k^{OM}+\dot{Y}_k^{DI} \tag{16}$$

For simplicity, we assume that the value of $\dot{Y}_k$ is mainly associated with $\dot{Y}_k^{CO}$.

4. Total Annualized Cost

The total annualized cost is given by the sum of the operating costs over the relevant devices plus the sum of the annualized capital costs (Eq. (17)). In addition, taxes related to greenhouses emissions have been considered

$$\text{TAC=Operation Cost (with considering emission taxes)} + \text{Capital Cost} \tag{17}$$

where,

TAC=Total Annualized Cost ($/y)

4-1. Modeling of Operating Costs

The utility prices can fluctuate rather quickly and the estimation of operating costs may be very different from a year to year. It is

highly unrealistic to expect constant prices for utilities in the future. Nemet et al. [48] considered the full lifetime of the HEN and future utility prices.

In this paper, the developed model based on the trends of historical prices has been considered for estimation of operating costs, where the annual utility cost with varying prices is calculated for every period during the lifetime as [48,49]:

$$C_{tot}^{Op} = \Sigma_t (C_t^{Op} \cdot f_t) \cdot t_{Op}^{tot} \quad (18)$$

Further economic data can be found in Refs. [48-51].

4-2. Modeling of Capital Costs

The basis for calculating the overall capital expenditure of the plant is the purchase cost of the equipment. The most significant cost is assumed contributed by the turbine and the boiler.

The purchase cost of a boiler mainly depends on its design steam flow rate and pressure, as these parameters define the amount and specifications for the materials of construction. Eq. (19) represents a linear formulation to relate the purchase cost of a boiler to its design steam flow rate and pressure.

$$PC_{bol} = A * M_{stm\text{-}D} + B \quad (19)$$
$$A = 0.249 * P_{bol} + 47.19$$
$$B = 3.29 * P_{bol} + 624.6$$

where,

PC_{bol}: Boiler purchase cost (1000 $) (2002)

A, B: Regression coefficients for the purchase function (1000 $/(kg/s), 1000 $)

P_{bol}: Boiler steam design pressure (bar)

$M_{stm\text{-}D}$: Boiler design steam flow (kg/s)

We used two functions to estimate the purchase cost of a steam turbine. First function is based on Aguilar cost function [52], which represents an equation to estimate the purchase cost of a steam turbine to its design steam flow rate and volumetric flow passing through the unit (Eq. (20)):

$$PC_{st} = 474.5 * Vol + 1111.7 \quad (20)$$
$$VOI = M_{st} * \sqrt{\nu_{in} * \nu_{out}}$$

where,

PC_{st}: Steam turbine purchase cost (without including electric generator) (1000 $) (2002)

VOl: Average steam volumetric flow rate passing through turbine (m^3/s)

M_{st}: Design steam turbine mass flow rate (kg/s)

v_{in}: Specific volume of the steam entering the turbine (m^3/kg)

v_{out}: Specific volume of the steam discharged by the turbine (m^3/kg)

Second function is based on Al-Azri [40] equipment cost function that represents an equation to estimate the purchase cost of a steam turbine to its design shaft power output (Eq. (21)).

$$PC_{st} = 475 * (W * 2.93E\text{-}04)^{0.45} \quad (21)$$

where,

W: the turbine shaft power output (kW)

Eq. (22) represents an equation to estimate the purchase cost of an electric generator to its design output.

$$PC_{gen} = 0.0414 * W_{gen} + 190.49 \quad (22)$$

where,

PC_{gen}: Purchase cost for electric generators (1000 $)

W_{gen}: Design output for electric generators (kW)

Eq. (23) represents an equation to estimate the purchase cost of a deaerator.

$$PC_{dea} = 0.958 * M_{dea} + 30.0 \quad (23)$$

where,

PC_{dea}: Deaerator purchase cost (1000 $) (2002)

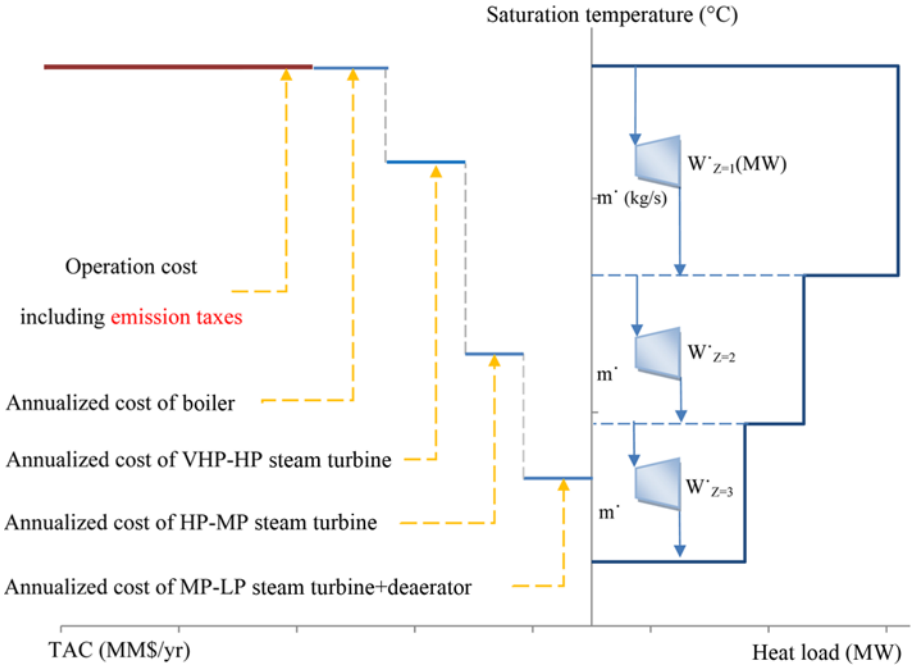

Fig. 5. Schematic of the utility system layout on modified SUGCC.

M_{dea}: Design water mass flow from the deaerator (kg/s)

In addition, it is possible to update these functions employing the Chemical Engineering Plant Cost Index (CEPCI) [51] factor corresponding to the ratio of the actual index over the base year one.

The capital cost of the component is converted to annualized cost by using the capital recovery factor CRF (i, n) (Eq. (24))

$$CRF = \frac{i(1+i)^n}{(1+i)^n - 1} \quad (24)$$

where,

i: Interest rate

n: Specified plant life

5. Graphical Representations

The other form of SUGCC has been applied to demonstrate on the same diagram heat recovery through the steam mains, steam generation and used, boiler steam demand, shaft work production, total annualised cost with considering emission's taxes, actual temperature of steam mains and steam flow rate. As shown in Fig. 6, the left side of the horizontal axis demonstrates the TAC with considering taxes for site utility, and the right side of horizontal axis shows the heat demand of the steam mains and steam demand of boiler and potential for power generation. Furthermore, it is helpful to display the system information graphically to visualize the TAC with considering of utility system and shaft work production.

In addition, fixed steam headers, such as assumed in total site analysis, give no allowance for reheating before turbine expansion, which can be valuable to consider when optimizing the steam system for certain plant configurations. Additionally, previous work focused on the steam pressure level based on its saturation temperature alone. The present work examines the effect of including both sensible and latent heating of steam in the Extended SUGCC (ESUGCC). It demonstrates that including sensible heating allows for better thermal matching between the process and steam system which results in improving the overall efficiency while minimizing cost.

As shown in Fig. 6, the right side of new curve illustrates a thermodynamic expansion of steam at steam network on a Temperature-Entropy diagram. Point 1 determines actual temperature of steam at outlet of the boiler and points 2, 3 and 4 show actual temperature of steam at outlet of the VHP-HP, HP-MP and MP-LP turbines.

CASE STUDIES

To show the applicability of the new procedure in the total site analysis, two case studies were considered.

1. Case Study 1

In the first case study, the four considered steam levels were very high pressure (VHP), high pressure (HP), medium pressure (MP) and low pressure (LP) at 120, 50, 14 and 3 bar. The heat demand at HP, MP and LP steam levels was 50, 40 and 85 MW. The data parameters related to steam levels were specified as given in Table 3.

Fig. 7 shows the necessary input data for cogeneration targeting

Table 3. Data parameters for case study 1

	VHP	HP	MP	LP
Pressure (bara)	120	50	14	3
Saturation temperature (°C)	324	264	195	133
Net heat load (MW)	0	50	40	85

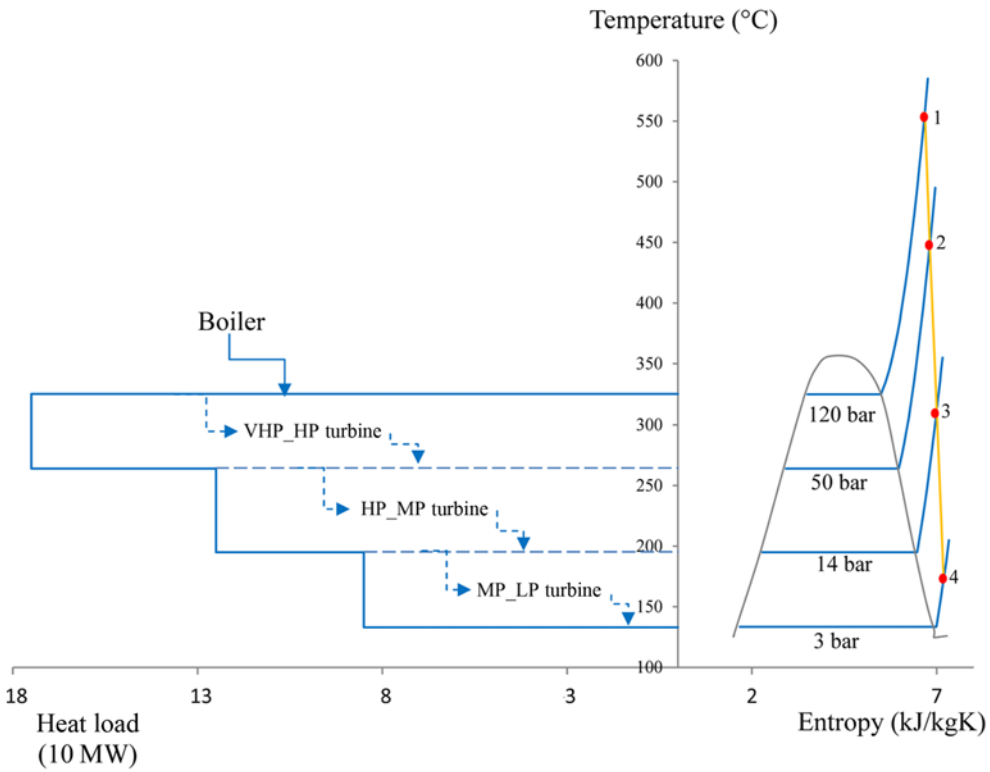

Fig. 6. Schematic of ESUGCC.

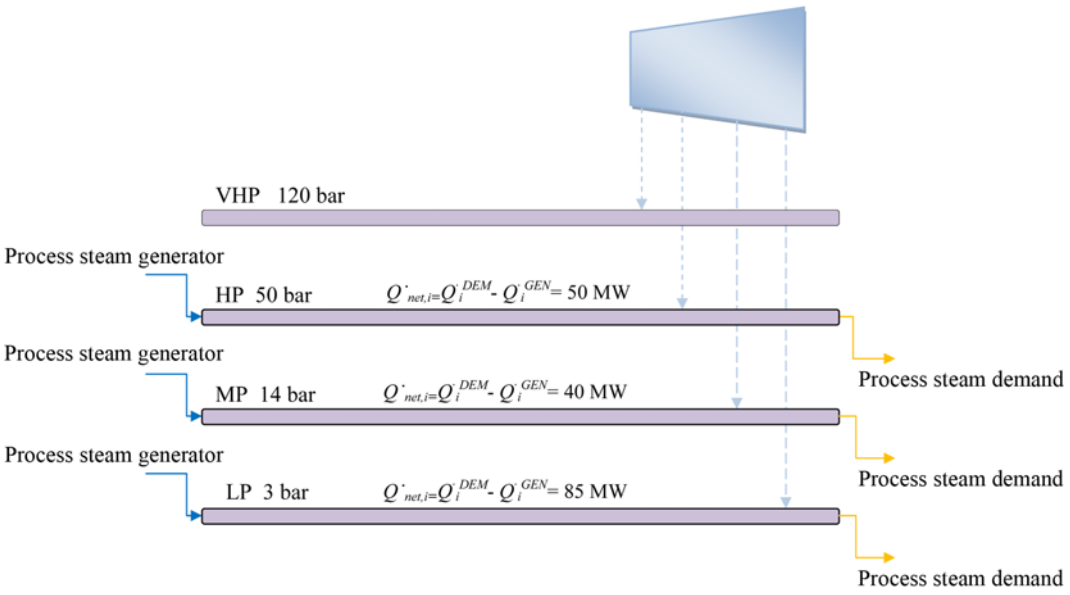

Fig. 7. Total site utility system for case study 1.

of the site utility system related to case study 1 [10,11].

In this case, the water supplied to the boiler was assumed to be at 105 °C and the superheat in LP was assumed to be 40 °C. Also, it was assumed that the total area available, municipality was 3.85E+11 m^2 and total water resources, municipality was 390873.72 m^3 for footprint evaluation.

2. Case Study 2

In the second case study, the four considered steam levels were very high pressure (VHP), high pressure (HP), medium pressure (MP) and low pressure (LP) at 90, 46, 15.5 and 2.7 bar. The heat demand at MP and LP steam levels was 6.88 and 16.25 MW, and, in this case, the process steam generation at HP level was higher than the process steam demand, and heat surplus at HP steam level was 10.63 MW. The data parameters for each level are specified as given in Table 4.

Table 4. Data parameters for case study 2

	VHP	HP	MP	LP
Pressure (bara)	90	46	15.5	2.7
Saturation temperature (°C)	303	259	200	130
Net heat load (MW)	0	−10.63	6.88	16.25

Fig. 8 shows the necessary input data for cogeneration targeting of the site utility system related to case study 2 [10,11].

It was assumed that the water supplied to the boiler was at 105 °C

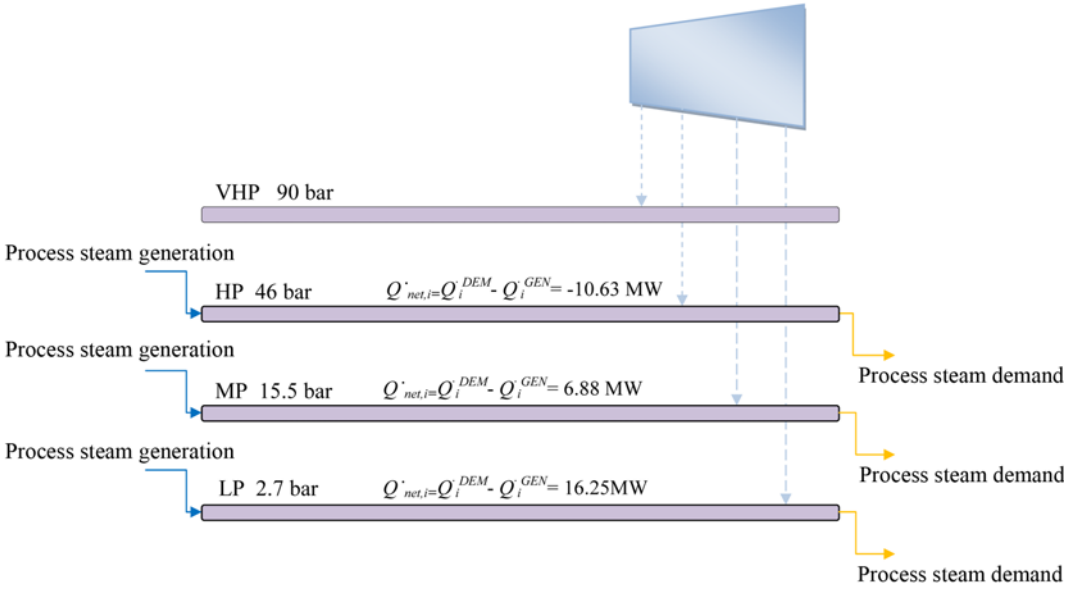

Fig. 8. Total site utility system for case study 2.

and the degree of superheat in LP was assumed to be 20 °C. Also, it was assumed that the total area available, municipality was 1.9E+10 m^2 and total water resources, municipality was 28,806 m^3 for footprint analyses.

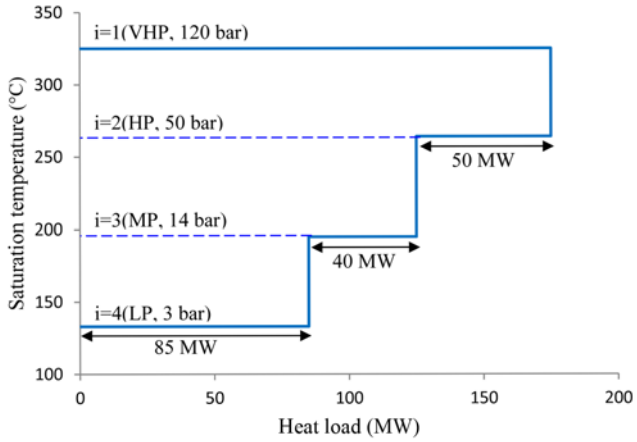

Fig. 9. The SUGCC of case study 1.

RESULTS

The SUGCC of the first case study is shown in Fig. 9. It presents a schematic of the shaft power target in the second case study. The right side shows a thermodynamic expansion of steam at steam network on a temperature-entropy diagram.

The extended SUGCC (ESUGCC) of case 1 is demonstrated in Fig. 10. Point 1 shows the actual temperature of the steam at the outlet of the boiler, and points 2, 3 and 4 indicate the actual temperature of steam at outlet of the VHP_HP, HP_MP and MP_LP turbines. Also, Table 5 determines the shaft power targeting results from the main cogeneration targeting.

As shown in Table 5, the total power target of 34.1 MW from IBTM methodology was significantly different from the detailed design procedure of 38.1 MW with an error of 10.5%. The shaft work target obtained from the THM model of 14.1 MW was 63% different from the shaft work obtained from the detailed design procedure. Similarly, the SHM model target was 8.73%, different from

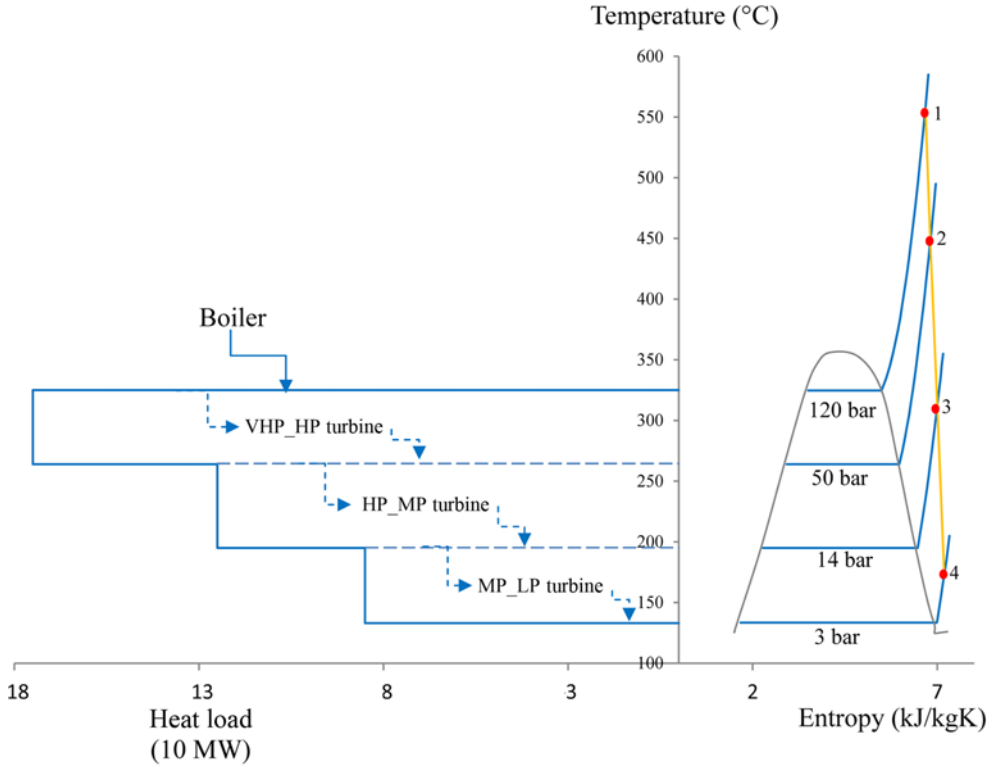

Fig. 10. The extended SUGCC (ESUGCC) of steam network- case 1.

Table 5. Shaft power targeting results for case study 1

Methodology	Error %	Total (MW)	'VHP-HP' (MW)	'HP-MP' (MW)	'MP-LP' (MW)
IBTM	−10.50	34.100	13.490	12.28	8.330
THM-model in STAR	−63.00	14.100	9.400	4.700	0
SHM	+8.99	41.430	18.200	14.460	8.770
New method	−0.352	37.970	14.740	13.520	9.710
STAR simulation	−0.344	37.973	14.740	13.520	9.710
Thermoflow simulation	-	38.104	14.797	13.558	9.749

the actual shaft work from the detailed design procedure. These discrepancies in the shaft work targets were due to the assumptions used in these models. The shaft work target obtained from the new method of 37.97 MW was only 0.35% different from the detailed design procedure in THERMOFLOW [53] and was only 0.0079% different from the STAR Software [54]. The levelized cost of each components was computed considering an interest rate i=5% and a plant expected life n=20 year with annual operating time of 8,000 h/yr.

Three cost functions were considered for case study 1. The first one was related to Aguilar [52]. The second one is based on Al-Azri [40] steam turbine cost function and the third one is based on THERMOFLOW software.

With considering steam turbine cost function based on Aguilar

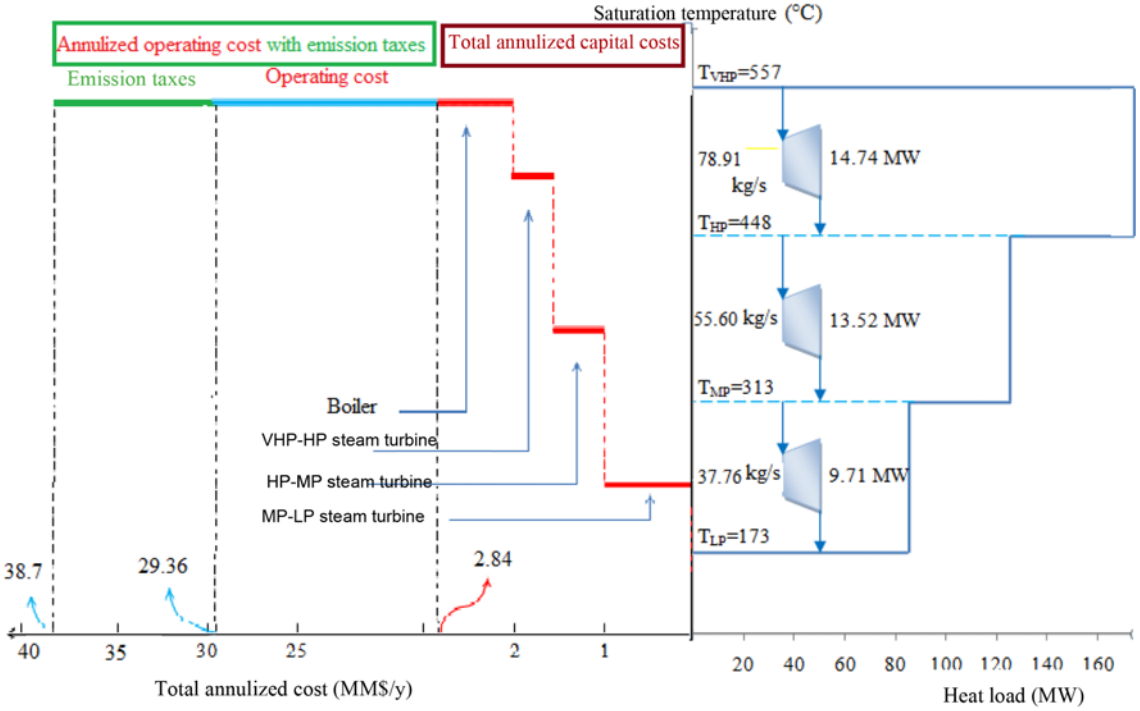

Fig. 11. TAC with considering emission taxes and cogeneration potential based on Aguilar (2005) steam turbine cost function (case study 1).

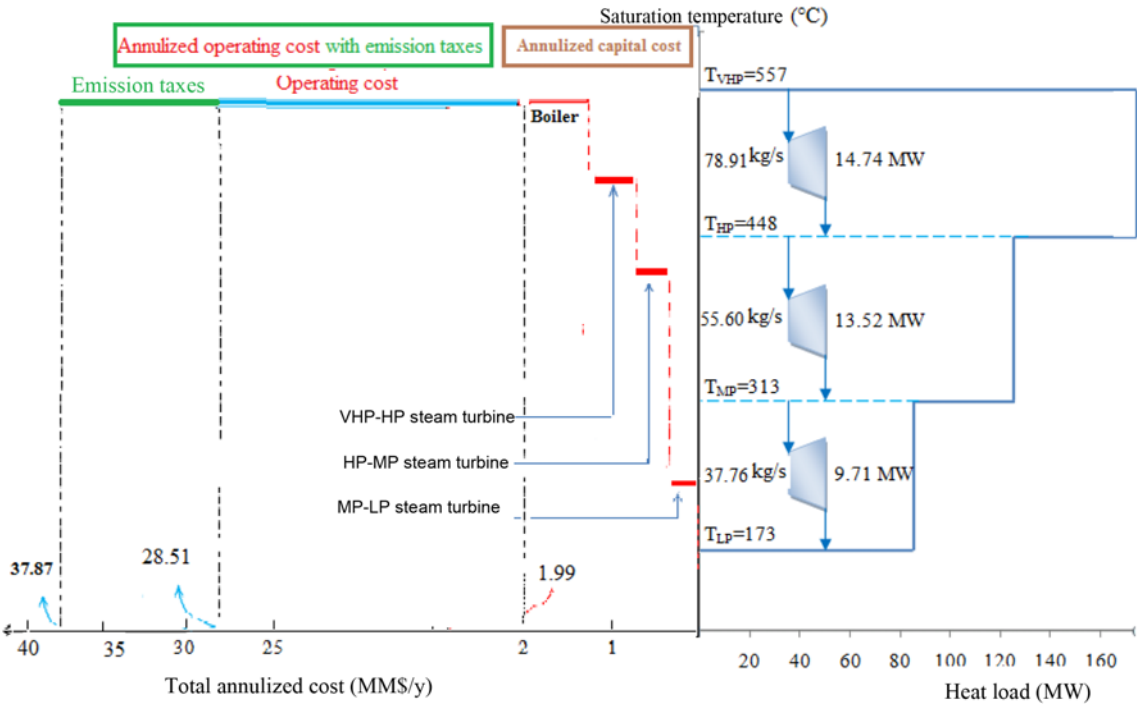

Fig. 12. TAC with considering emission taxes and cogeneration potential based on Al-Azri (2008) steam turbine cost function (case study 1).

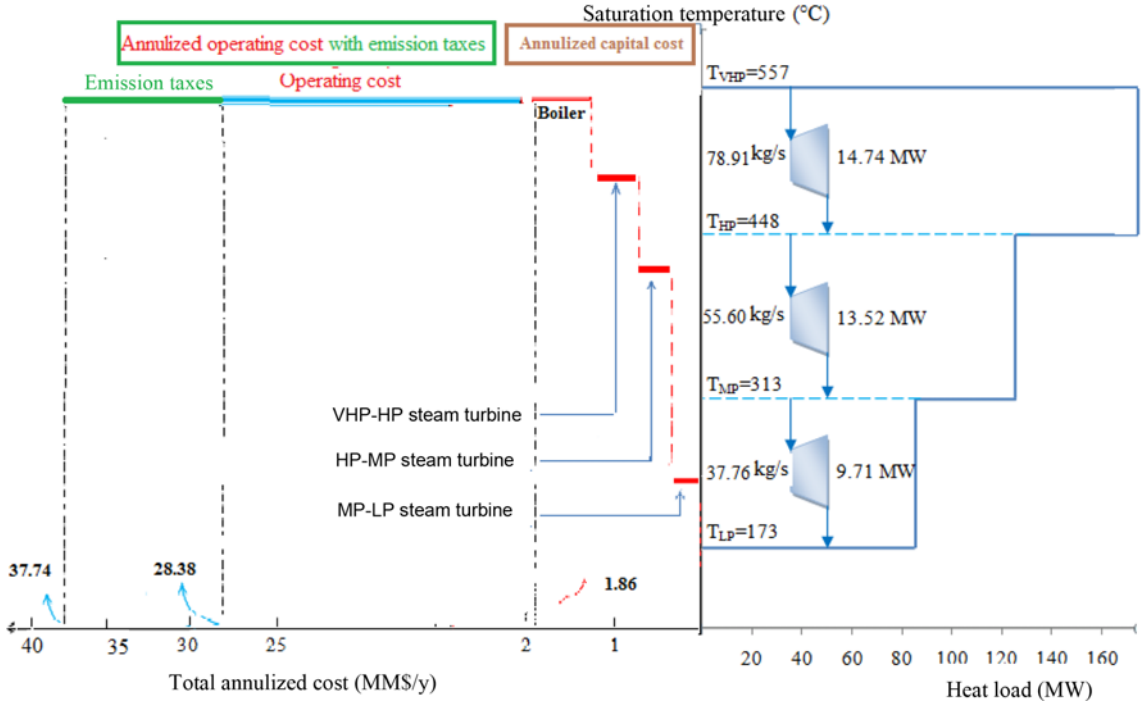

Fig. 13. TAC with considering emission taxes and cogeneration potential based on THERMOFLOW (case study 1).

[52] relations, TAC with considering emission taxes and cogeneration potential obtained are demonstrated in Fig. 11.

In addition, based on cost functions of Al-Azri (2008) [40] TAC including emission taxes and cogeneration potential obtained from proposed procedure are illustrated in Fig. 12.

Finally, the schematic illustration of shaft power target and TAC in the first case study based on THERMOFLOW [53] steam turbine cost function is shown in Fig. 13.

The SUGCC of the second case study is shown in Fig. 14. The extended SUGCC (ESUGCC) of steam network has been demonstrated in Fig. 15. As shown in Table 6, the total power target of 4.4 MW from the IBTM methodology was significantly different from the detailed design procedure of 4.524 MW with an error of 2.74%. The shaft work target obtained from the THM model of 4.200 MW was 7.16% different from the shaft work obtained from the detailed design procedure. Similarly, SHM model target was 19.36% different from the actual shaft work from the detailed design procedure. These discrepancies in the shaft work targets were due to the assumptions used in these models. The shaft work target obtained from the new method of 4.520 MW was only 0.088% different from the detailed design procedure in THERMOFLOW [53] and was only 0.022% different from the STAR Software [54].

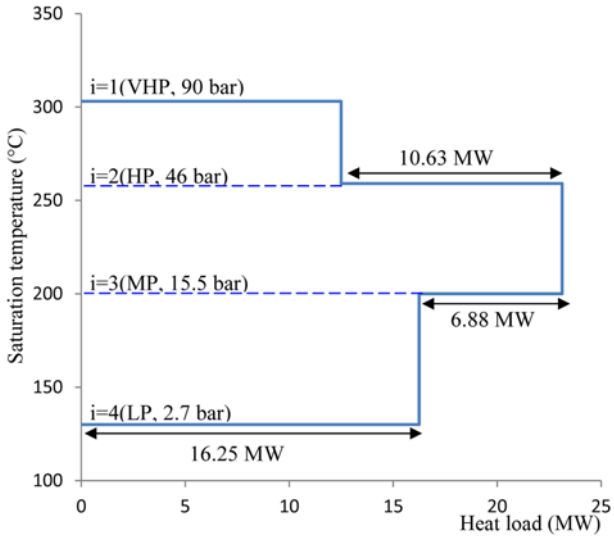

Fig. 14. The SUGCC of case study 2.

The levelized cost of components was calculated considering an interest rate i=5% and a plant expected life n=20 year with annual

Table 6. Shaft power targeting results for case study 2

Methodology	Error %	Total (MW)	'VHP-HP' (MW)	'HP-MP' (MW)	'MP-LP' (MW)
IBTM	−2.91	4.520	0.80	1.9	1.70
THM [Model in STAR]	−7.33	4.400	0.50	1.9	1.80
SHM	19.15	4.200	1.80	1.9	1.70
New method	−0.26	5.400	0.57	2.0	1.95
STAR simulation	−0.22	4.521	0.57	2.0	1.951
Thermoflow simulation	-	4.524	0.571	2.001	1.952

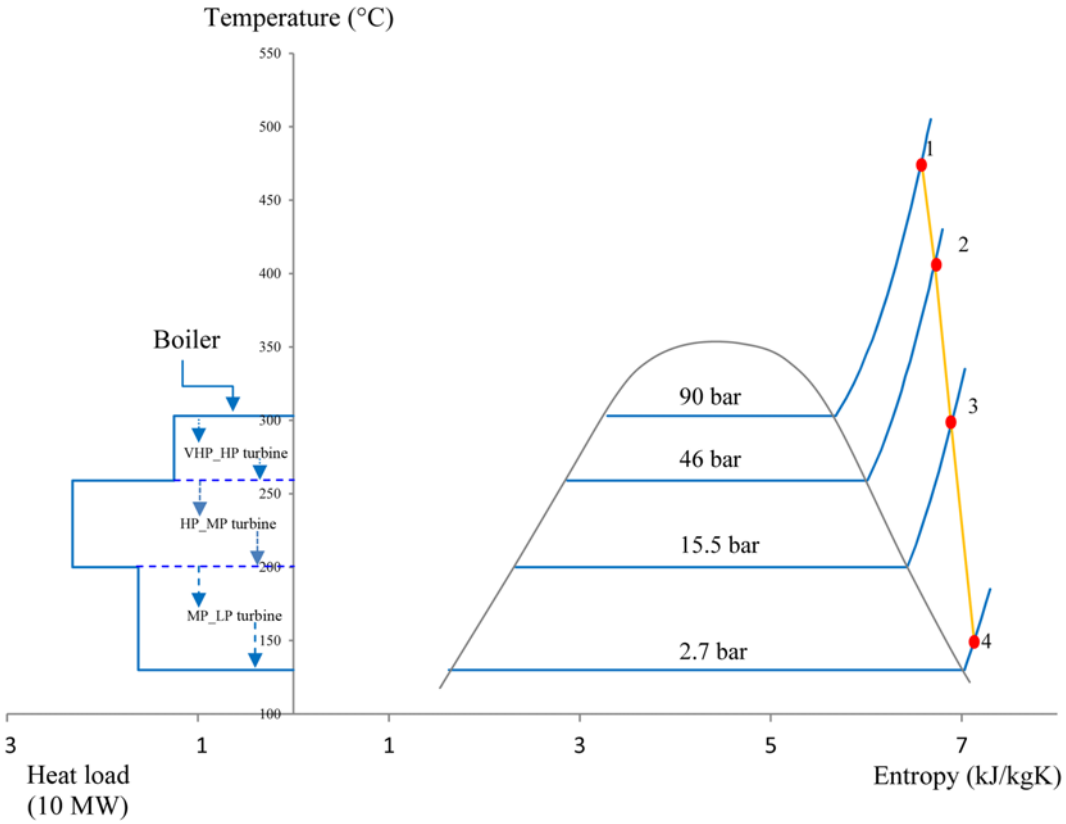

Fig. 15. The extended SUGCC (ESUGCC) of steam network-case 2.

operating time of 8,000 hr/yr.

Two cost functions were considered for case study 2. The first one is related to Aguilar [52] and the second one is based on Al-Azri [40] steam turbine cost functions.

In this respect, Figs. 16 and 17 demonstrate a schematic illustration of shaft power target and TAC with considering emission taxes

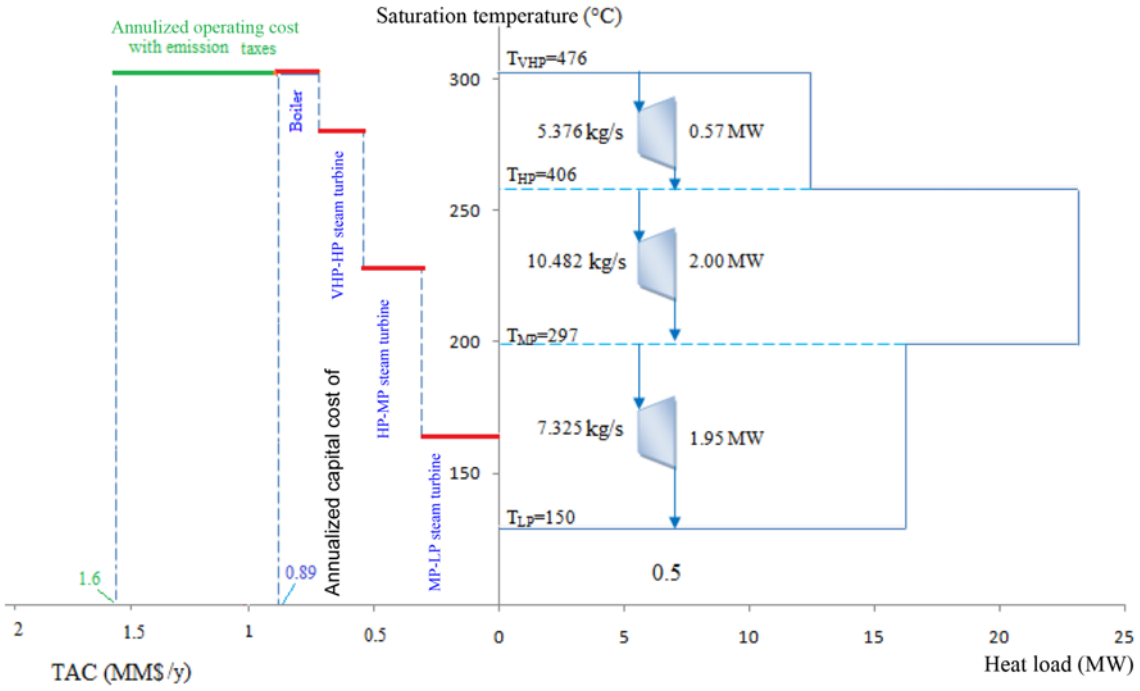

Fig. 16. TAC with considering emission taxes and cogeneration potential based on Aguilar (2005) steam turbine cost function (case study 2).

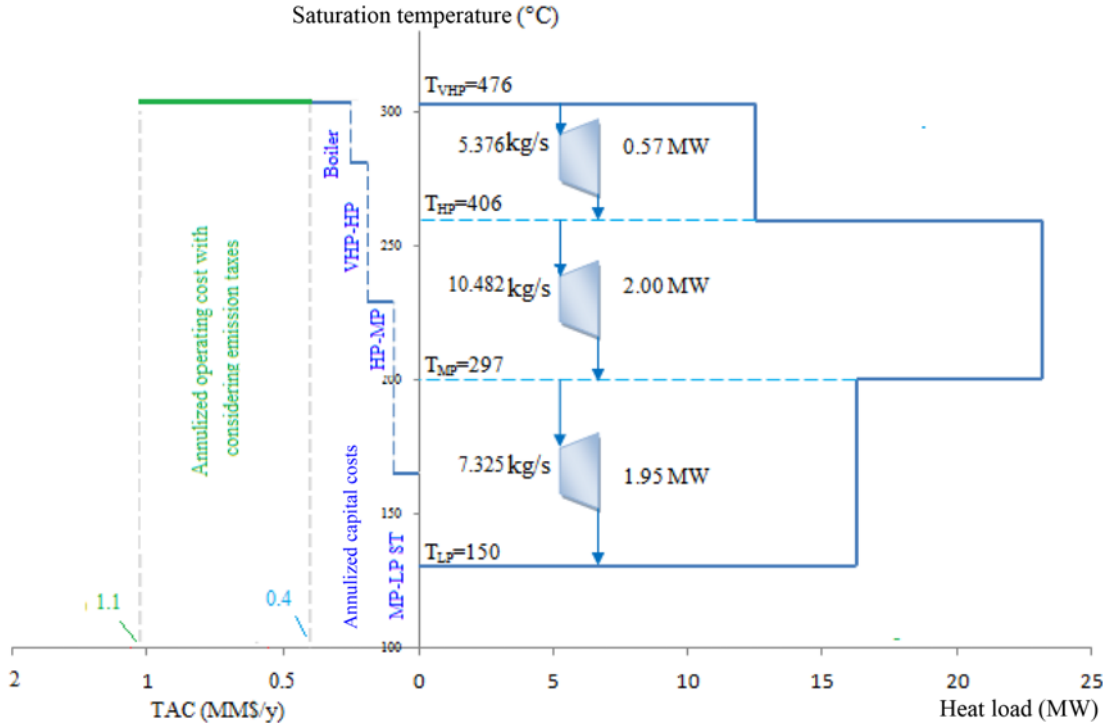

Fig. 17. TAC with considering emission taxes and cogeneration potential based on Al-Azri (2008) steam turbine cost function (case study 2) case 1.

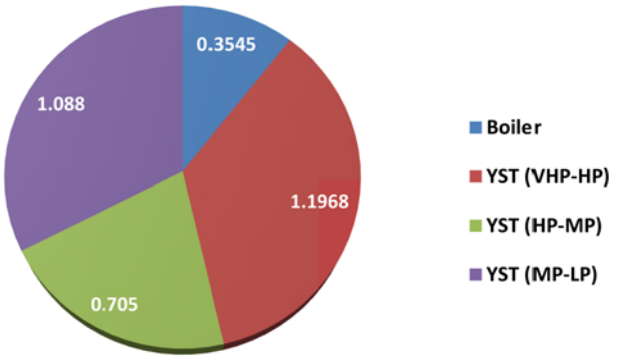

Fig. 18. Distrubuation of Y (Pts/h) for each component - case 1.

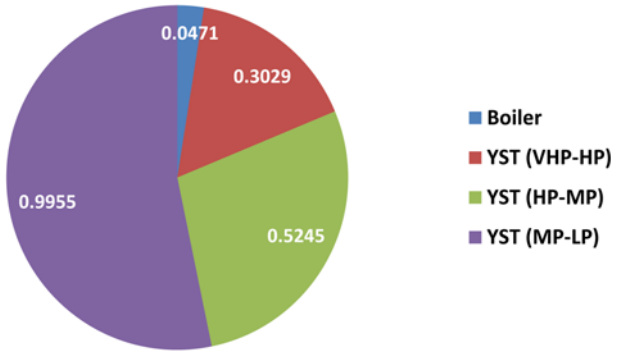

Fig. 19. Distrubuation of Y (Pts/h) for each components - case 2.

in the second case study based on Aguilar [52] and Al-Azri [40] steam turbine cost functions.

In addition, the distribution of eco-indicator 99 (Y) for each component of site utility in case 1 and case 2 is shown in Fig. 18 and Fig. 19. As shown in Fig. 18, the highest Y value was related to VHP-HP steam turbine and lowest Y was related to boiler in case 1. Also, the highest value for Y was related to MP-LP steam turbine and the lowest Y was related to boiler in case 2. In addition, the Y-SUGCC representations for case 1 and case 2 were demonstrated in Fig. 20 and Fig. 21. The footprint values for case study 1 are determined in Table 7. The environmental strategy map for case study 1 is demonstrated in Fig. 22. As shown, the carbon footprint was lowest and energy footprint was highest values. The total area available, municipality for case 1 was 3.85E+11 m^2 and total water resources, municipality was 390,873.72 m^3.

In addition, the footprint values calculated for case 2 are shown in Table 8. The environmental strategy map for case 2 is illustrated in Fig. 23. Results demonstrate that the highest footprint for case study 2 was related to energy and lowest related to carbon same as case 1. The total area available, municipality for case 2 is 1.9E+10 m^2 and total water resources, municipality was 28,806 m^3.

CONCLUSION

A new environmental targeting procedure was developed that provides a consistent, general procedure for determining the mass flowrates and the efficiencies of the used turbines. This algorithm utilizes the relationship of entropy with enthalpy and isentropic efficiency. In adition, the new procedure allows for targeting shaftwork production, degree of superheat in the steam boiler with a high level of accuracy and estimation of GHG and TAC with considering emission taxes. Furthermore, the new procedure can target carbon, water,

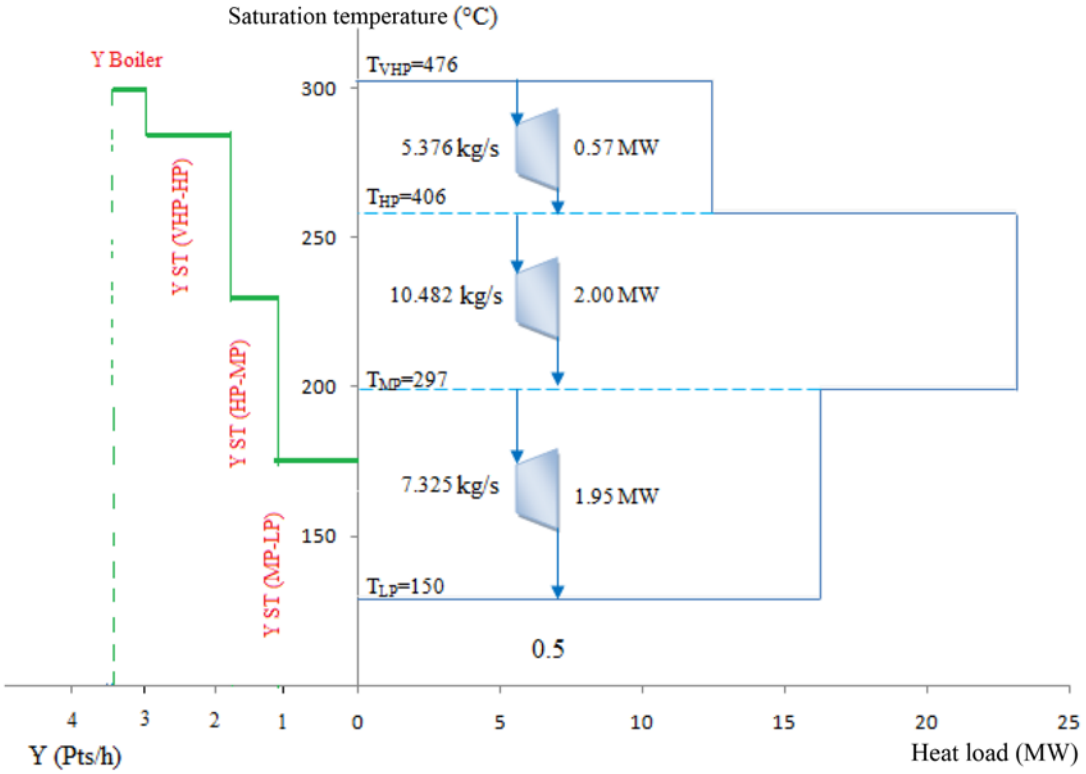

Fig. 20. Y-SUGCC for case study 1.

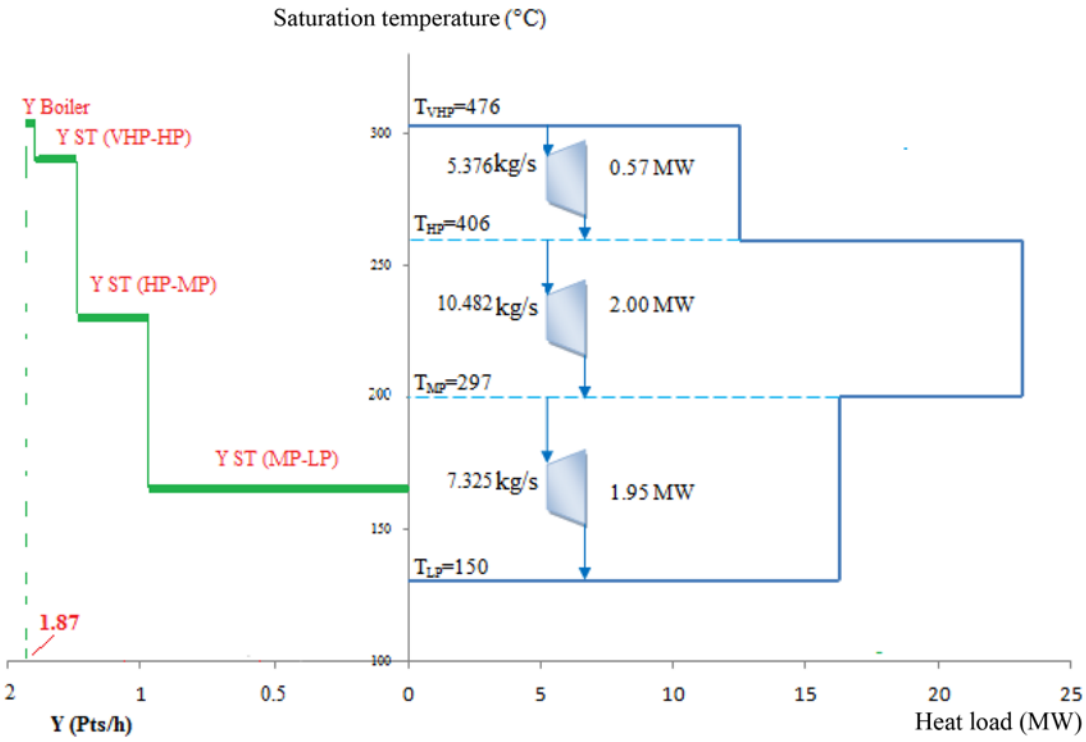

Fig. 21. Y-SUGCC for case study 2.

energy and emission footprints and eco-indicatore 99. In this regard, a new representation Y-SUGCC has been propsed. Also, the extended SUGCC (ESUGCC) has been introduced.

The developed methodology is required to be further extended to accommodate the integration of renewable energy sources, such as solar, wind, etc. for the total site with high accuracy. Another work which could be considered in future is to optimize steam levels for reducing the overall energy consumption for the site. Moreover, a new

Table 7. Footprint evaluation for case study 1

Parameters	Value
Carbon footprint (m^2)	1,228,091
Emission footprint (m^2)	26,337,527,415
Energy footprint (m^2)	166,206,621,545
Water footprint (m^3)	97,718

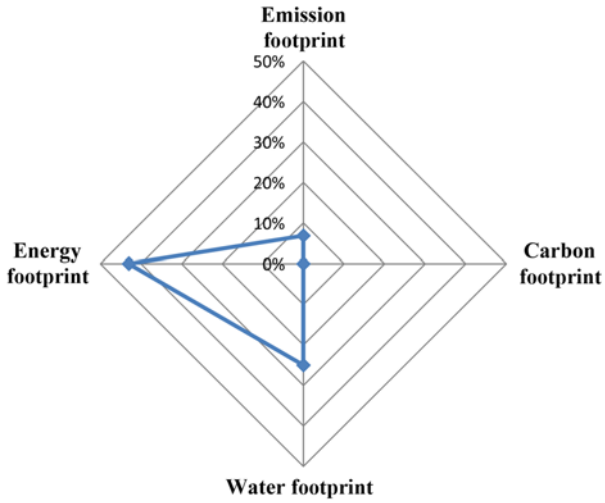

Fig. 22. Environmental strategy map for case study 1.

Table 8. Footprints evaluation for case study 2

Parameters	Value
Carbon footprint (m^2)	78,986
Emission footprint (m^2)	9,050,579,750
Energy footprint (m^2)	10,689,768,737
Water footprint (m^3)	6,625

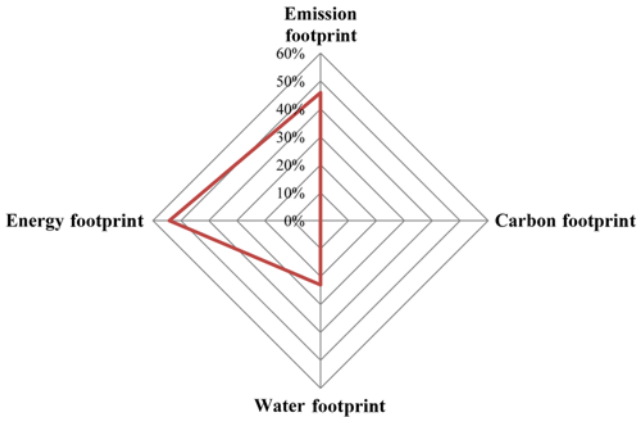

Fig. 23. Environmental strategy map for case study 2.

environmental targeting strategy developed in this work can be used for the heat recovery of low-grade waste heat in process industries.

NOMENCLATURE

h : specific enthalpy [kJ/kg]
$\dot{m}$: mass flow rate [kg/s]
P : pressure [bar]
$\dot{Q}$: heat load [MW]
s : specific entropy [kJ/kgK]
T : temperature [°C]
TAC : total annualized cost
W : shaft work [MW]
SUGCC : site utility grand composite curve
LCA : life cycle assessment
CEPA : carbon emission pinch analysis
TSST : total site sensitivity table
TS-PTA : total site problem table algorithm
PTA : problem table algorithm
TSUD : total site utility distribution table
CF : carbon footprint
EMF : emission footprint
F_{CO_2} : the fraction of CO_2 absorbed by the oceans
M_{CO_2} : product specific emission of CO_2
S_{CO_2} : sequestration rate of CO_2 by biomass
EF : the equivalence factor for forests

Greek Symbol
η : isentropic efficiency

Subscripts
is : isentropic
Sat : saturated conditions

Superscripts
DEM : process steam demand
GEN : process steam generation
i : steam main
net : net heat or mass load

REFERENCES

1. V. R. Dhole and B. Linnhoff, *Comput. Chem. Eng.*, **17**, 101 (1993).
2. K. Raissi, *Total site integration*, PhD Thesis, UMIST, Manchester (1994).
3. J. Klemes, V. R. Dhole, K. Raissi, S. J. Perry and L. Puigjaner, *Appl. Thermal Eng.*, **17**(8-10), 993 (1997).
4. M. Sorin and A. Hammache, *Appl. Thermal Eng.*, **25**, 961 (2005).
5. S. P. Mavromatis and A. C. Kokossis, *Chem. Eng. Sci.*, **53**(8), 1585 (1998).
6. D. A. Harell, *Resource conservation and allocation via process integration*, Ph.D. Thesis, Texas A&M University (2004).
7. P. S. Varbanov, S. Doyle and R. Smith, *Chem. Eng. Res. Design*, **82**(5), 561 (2004).
8. T. Mohan and M. M. El-Halwagi, *Clean Technol. Environ. Policy*, **9**(1), 13 (2007).
9. J. M. Medina-Flores and M. Picón-Núñez, *Chem. Eng. Sci.*, **65**(9), 2811 (2010).
10. S. Bandyopadhyay, J. Varghese and V. Bansal, *Appl. Thermal Eng.*, **30**, 6 (2010).
11. A. Ghannadzadeh, S. Perry and R. Smith, *Chem. Eng. Transactions*, **25**, 917 (2011).
12. A. Ghannadzadeh, S. Perry and R. Smith, *Appl. Thermal Eng.*, DOI:

10.1016/j.applthermaleng.2011.10.006 (2011).
13. A. Kapil, I. Bulatov, R. Smith and J.-K. Kim, *Chem. Eng. Res. Design*, DOI:10.1016/j.cherd.2011.09.001 (2010).
14. P. S. Varbanov and J. Klemes, *Comput. Chem. Eng*., **35**, 1815 (2011).
15. P. Y. Liew, S. R. Wan Alwi, P. S. Varbanov, Z. A. Manan and J. Klemes, *Appl. Thermal Eng.*, **40**, 397 (2012).
16. P. S. Varbanov, Z. Fodor and J. J. Klemeš, *Energy*, DOI:10.1016/j.energy.2011.12.025 (2012).
17. Z. Fodor, J. Klemes, P. S. Varbanov, M. R. W. Walmsley, M. J. Atkins and T.Walmsley, *Chem. Eng. Transactions*, **29**, 409 (2012).
18. R. Hackl and S. Harvey, *Chem. Eng. Transactions*, **29**, 73 (2012).
19. N. E. Mohammad Rozali, S. R. Wan Alwi, Z. Abdul-Manan and J. J. Klemeš, *Chem. Eng. Transactions*, **29**, 121 (2012).
20. A. Nemet, J. Klemes and Z. Kravanja, *Energy*, **45**, 264 (2012).
21. W. Tjan, R. R. Tan and D. C. Y. Foo, *J. Cleaner Production*, **18**, 848 (2010).
22. EPA, Environmental Protection Agency. http://www.epa.gov/climatechange/ (accessed APRIL 2012).
23. M. Gadallaa, Z. Olujic, P. Jansens, M. Jobson and R. Smith, *Environ. Sci. Technol.*, **39**(17) (2005).
24. I. Dincer and M. A. Rosen, Exergy: energy, environment and sustainable development, Elsevier (2007).
25. G. Stupara, D. Tucakovia, T. Živanovia, M. Banjaca, S. Beloševib, V. Beljanskib, I. Tomanovib, N. Crnomarkovib and M. Sijerib, *The influence of primary measures for reducing NO_x emissions on energy steam boiler efficiency*, Proceedings of ECOS 2012 - the 25th International Conference on Efficiency, Cost, Optimization, Simulation and Environmental Impact of Energy Systems, (125) 1-13, June 26-29, 2012, Perugia, Italy (2012).
26. International Organization for Standardization (ISO): Environmental management—life cycle assessment. European Standard ENISO14040 and 14044, Geneva (2006).
27. J. Dewulf and H. Van Langenhove, *Environ. Sci. Pollut. Res*., **9**(4), 267 (2002).
28. R. R. Tan and D. C. Y. Foo, *Energy*, **32**, 1422 (2007).
29. M. J. Atkins, A. S. Morrison and M. R. W. Walmsley, *Appl. Energy*, **87**, 982 (2010).
30. D. Crilly and T. Zhelev, *Energy*, **33**, 1498 (2008).
31. D. Crilly and T. Zhelev, *An emergy-based targeting technique for treatment and utilisation of greenhouse gas emissions*, In: Novosad, J. (Ed.), Paper Presented in the 18th International Congress of Chemical and Process Engineering (CHISA) - Summary 4: PRES 2008 and System Engineering, **4**, 1214 (2008).
32. S. Bandyopadhyay, D. C. Y. Foo and R. R. Tan, *AIChE J.*, **56**(5), 1235 (2009).
33. S. C. Lee, D. K. S. Ng, D. C. Y. Foo and R. R. Tan, *Appl. Energy*, **86**, 60 (2009).
34. R. R. Tan, D. C. Y. Foo and D. K. S. Ng, *J. Cleaner Production*, **17**(10), 940 (2009).
35. W. Tjan, R. R. Tan, D. C. Y. Foo, *J. Cleaner Production*, **18**, 848 (2010).
36. L.Cucek, J. Klemes and Z. Kravanja, *J. Cleaner Production*, **34**, 9 (2012).
37. R. E. H. Ooi, D. C. Y. Foo, D. K. S. Ng and R. R. Tan, *Chem. Eng. Transactions*, **29**, 415 (2012).
38. L. Èuèek, P. S. Varbanov, J. J. Klemeš and Z. Kravanja, *Chem. Eng. Transactions*, **29**, 61 (2012).
39. J. Klemes, F. Friedler, I. Bulatov and P. Varbanov, *Sustainability in the process industry: integration and optimization*, McGraw-Hill, New York (2010).
40. N. A. AL-Azri, *Integrated approaches to the optimization of process-utility systems*, Ph.D. Thesis, Texas A&M University (2008).
41. R. Smith, Chemical Process Design and Integration, Wiley, West Sussex (2005).
42. C. Monfreda, M. Wackernagel and D. Deumling, *Land Use Policy*, **21**, 231 (2004).
43. M. A. J. Hujbregts, S. Hellweg and R. Frischknecht, *Ecological Economics*, **64**, 798 (2008).
44. L. D. Benedetto and J. Klemes, *J. Cleaner Production*, **17**, 900 (2009).
45. L. Meyer, G. Tsatsaronis, J. Buchgeister, L. Schebek, *Energy Int. J.*, **34**, 75 (2009).
46. A. Boyano, A. M. Blanco-Marigorta, T. Morosuk and G. Tsatsaronis, *Energy Int. J*., DOI:10.1016/j.energy.2010.05.020 (2010).
47. Sima Pro, User's Manual. Pre Consultants BV, Amersfoort (NL) (2007).
48. A. Nemet, J. Klemes and Z. Kravanja, *Energy*, **45**, 264 (2012).
49. INDEX MUNDI, www.indexmundi.com/commodities/?commodity=petroleum-price-index (2012).
50. G. D. Ulrich and P. T. Vasudevan, How to Estimate Utility cost Chemical Engineering, www.che.com/technical_and_practical/2798.html (2006).
51. Chemical Engineering Economic Indicators, 2012. www.che.com/business_and_economics/economic_indicators.html.
52. Aguilar O. Design and optimization of flexible utility systems. PhD Thesis, The University of Manchester, Manchester, UK (2005).
53. GTPRO 18, Thermal Engineering Software for the Power Industry, Thermoflow, Inc., U.S.A. (2008).
54. STAR Software, Version 2, Center for Process Integration, School of Chemical Engineering & Analytical Science, University of Manchester, UK, Under license of K.N.Toosi University of Technology, Energy and Process Integration Laboratory.